Enhancing Acute Lymphoblastic Leukemia Image Segmentation: Unveiling the Impact of Color Spaces and Clustering Techniques

Sourav Banerjee*, Sudip Barik*, Jacob Tauro*, Debashis Das§, and Narayan C Debnath†
Kalyani Government Engineering College, India*
Meharry Medical College, USA §
Eastern International University, Vietnam†

Abstract

Leukemia, a cancer characterized by an excess of white blood cells, particularly Acute Lymphoblastic Leukemia (ALL), necessitates precise white blood cell (WBC) segmentation for computer-aided diagnosis. Despite the complex nature of WBC morphology and background, achieving accurate segmentation remains challenging. This paper explores contemporary WBC segmentation techniques, emphasizing clustering methods within ALL images, and highlighting the significance of suitable color spaces for cytoplasmic region segmentation. Additionally, it conducts a comparative evaluation of various color spaces and image clustering algorithms, with the aim of identifying the most effective combination for precise WBC segmentation.

Key words: Acute Lymphoblastic Leukemia (ALL), Clustering, Pathology Image, Image Segmentation, Color Spaces · White Blood Cell.

1 Introduction

1.1 The Role of Digital Pathology Images in Disease Diagnosis

Digital pathology images revolutionize disease diagnosis, with computer-aided diagnosis (CAD) providing efficient quantitative analysis. CAD mitigates observer discrepancies, emphasizing the importance of precise segmentation de- spite challenges such as noise and variations in cell characteristics [6, 9].

1.2 Acute Lymphocytic Leukemia and the Need for Accurate WBC Segmentation

Acute Lymphocytic Leukemia, also known as Acute Lymphoblastic Leukemia, is a severe hematological cancer that can quickly become fatal if not promptly treated. This disease predominantly affects children, with the highest incidence occurring between the ages of 2 and 5 years. Detecting this condition in its early stages is paramount, especially for children's well-being. The immature white blood cells (WBCs) associated with this condition are called lymphoblasts or blasts. These blast cells are categorized into three types based on their morphology: L1, L2, and L3, as per the FAB (French American-British) classification system [10]. Each category displays distinct shapes and patterns. L1 cells are characterized by their small size and uniform shape, accompanied by a minimal cytoplasmic portion. The nucleus is well-defined and circular. In contrast, L2 cells exhibit larger size and varying shapes. They have an asymmetrical nucleus and variable cytoplasmic area. L3 cells possess a circular or oval nucleus and are similar in size and shape. The nucleus contains vacuoles, and there's a noticeable cytoplasmic area. Generally, L3 cells are larger than L1 cells. Refer to Figure 1 for visual representations of L1, L2, and L3 cells.

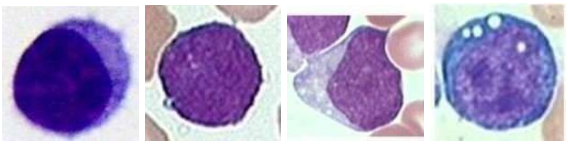

Fig. 1: Variability in morphology observed in blast cells as per the FAB classification. (a) Healthy lymphocytes cell; (b) L1-lymphoblasts Cell; (c) L2- lymphoblasts Cell; (d) L3-lymphoblasts Cell.

Accurate classification of these cell types offers vital insights to medical professionals, aiding them in formulating appropriate treatment plans. Hematologists perform differential white blood cell counts during blood tests to diagnose the disease [16]. However, this process is time-consuming, laborious, and expensive when done manually by experts. Furthermore, manual results might lack precision and reproducibility. Recent advancements have introduced automatic white blood cell classification technology with lower costs and enhanced accuracy, sparking interest in the field of hematological disease diagnosis.

The automated classification of white blood cells typically involves three main stages: segmentation, feature extraction, classification, and counting. It's evident that precise segmentation significantly influences the accuracy of

* Computer science and Engineering
§ Computer science and Engineering.
¶ School of Computing and Information Technology

classification and counting [16]. Hence, achieving accurate segmentation of white blood cells is paramount for the detection of Acute Lymphoblastic Leukemia. Numerous automated image segmentation techniques have been developed for early-stage Leukemia detection, including automatic thresholding [11], clustering [5], watershed [15], active contour [8], and deep learning [14]. Clustering, especially in various color spaces [18] (e.g., RGB, HSI, HSV, YCbCr, CIELAB), has shown promise for WBC segmentation. This study focuses on clustering- based WBC segmentation and aims to identify optimal color space and clustering technique combinations for precise ALL image segmentation. The following sections outline the structure of this paper: In Section 2, we provide detailed descriptions of the dataset used for White Blood Cell (WBC) segmentation. Section 3 elaborates on the clustering method employed, while Section 4 delves into the discussion of experimental results. Lastly, Section 5 offers concluding remarks, along with summaries, and outlines directions for future research.

2 Dataset Description

Two prominent publicly available datasets have been widely utilized in the academic literature for White Blood Cell (WBC) segmentation: the ALL-IDB Dataset [10]and the LISC Dataset [13]. These datasets are described in detail as follows:

ALL-IDB Dataset: The images contained within the ALL-IDB dataset were captured using a PowerShot G5 camera and were saved in JPG format, featuring a 24-bit color depth and a native resolution of 2592 x 1944 pixels. These images encompass a range of microscope magnifications, spanning from 300 to 500. The ALL-IDB database is categorized into two versions, specifically, ALL-IDB1 and ALL-IDB2, both designed to facilitate tasks related to segmentation and classification.

ALL-IDB1 constitutes a dataset comprising 108 images, which serves as a benchmark for the evaluation of segmentation and classification algorithms. Expanding upon this, ALL-IDB2 extends the capabilities of ALL-IDB1 and comprises 260 images, encompassing both normal and blast cells, with half of them representing lymphoblasts. It's worth noting that the grey-level characteristics of the images in ALL-IDB2 align with those found in ALL-IDB1.

LISC Dataset: The LISC Dataset comprises 400 color images of stained peripheral blood samples from 8 healthy subjects. These images were taken using a light microscope with a 100x magnification and saved in BMP format with a resolution of 720x576 pixels. The dataset comes from research centers in Tehran, Iran, and includes various normal leukocyte types. Additionally, an expert has outlined nucleus and cytoplasm regions in some of the images, but only 250 images have manual annotations.

3 Clustering Methods

Clustering embodies a systematic process wherein data entities are amalgamated into distinct clusters, guided by the principles of fostering high intra- cluster similarities and minimal inter-cluster similarities. The pursuit of optimizing this arrangement is encapsulated in defined objective functions, as elucidated by reference [5]. Leveraging these functions, the quest for the optimal partition of a given dataset is undertaken through the lens of minimizing or maximizing relevant metrics. These objective functions often encapsulate intricate statistical-mathematical relationships linking individual data elements to the prospective representatives of each cluster, colloquially known as cluster centers [1]. An optimal partition, delineating entities into 'c' classes, necessitates adherence to a specific set of properties that uphold the structural integrity of the resulting clusters:

1. At least one data vector should be assigned to each cluster, i.e.,
$$c_i = \emptyset, \forall i \in \{1, 2, \ldots, c\} \quad (1)$$
2. There should be no data vector in common between two clusters, i.e.,
$$c_i \cap c_j = \emptyset, \forall i = j \text{ and } i, j \in \{1, 2, \ldots, c\} \quad (2)$$
3. Each data vector must be associated with a cluster, i.e.,
$$\sum_{i=1}^{c} U = D_v \quad (3)$$

Where, D_v is stands for total number of objects.

4 Experimental Results

The assessment of the proposed methodologies transpired across a comprehensive collection of a hundred images sourced from all IDB datasets. Within this evaluative framework, three widely acknowledged clustering algorithms, namely K-Means (KM), Fuzzy C-Means (FCM), and Self Organizing Map (SOM) were harnessed for the crucial task of segmentation. The vital parameters underpinning these distinct clustering techniques were meticulously selected as follows:

The selection of cluster prototype values varies according to the specific clustering algorithm: it is set to 5 for Fuzzy C-Means (FCM), 4 for K-Means (KM), and 3 for Self-Organizing Maps (SOM). In the case of FCM, we employ a fuzzification parameter of 2. The algorithms are designed to terminate when the maximum difference between two successive partition matrices U falls below predefined minimal error threshold η, which is mathematically represented as $\text{Max } U^{t} - U^{t+1} < \eta$, with η being set to 10^{-5}. For K-Means, the procedure halts when the change in centroid values becomes smaller than η.

This approach ensures that the clustering process terminates when the desired level of convergence or accuracy is achieved for each respective algorithm.

Figure 2 depicts the original images of several Acute Lymphoblastic Leukemia blast cells. The assessment of segmentation accuracy for the proposed models involves the use of seven performance evaluation parameters based on ground truth data. These parameters include Accuracy (AC) [12], Precision Index (PI) [7], Specificity Index (SI) [2], Recall Index (RI) [3], Dice Index (DI) (also referred to as F-score or F-measure or Dice similarity coefficient) [19], Jaccard Index (JI) [17], and Matthews's correlation coefficient (MCC) [4].

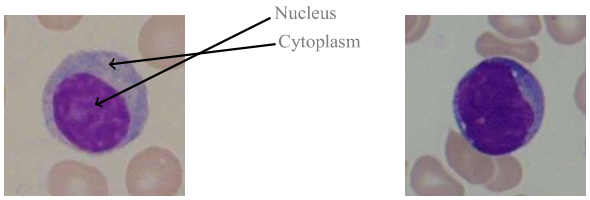

Fig. 2: Original Acute Lymphoblastic Leukemia images

4.1 Results over Nucleus Segmentation

This section evaluates nucleus segmentation using FCM, KM, and SOM across five color spaces. Tables 1 and 2 illustrate results for two images, while Tables 3,4,5 present average quality parameters of over 100 images. FCM and KM excel in CIE Lab, while SOM performs best in HSV and HSI, with SOM-HSV being the optimal pair.

Table 1: Segmenting Nuclei with Cluster Analysis in Various Color Spaces for Figure 2(a)

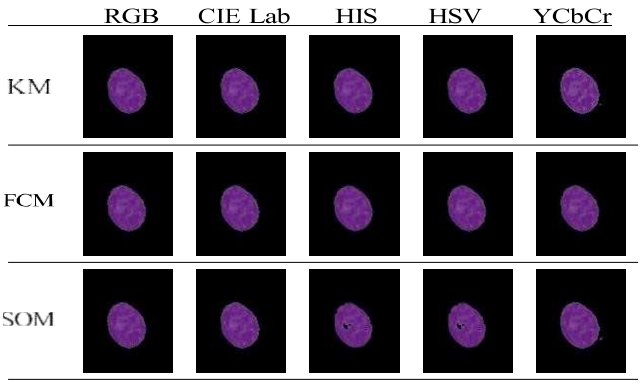

4.2 Results over Nucleus Segmentation

This section evaluates WBC (nucleus with cytoplasm) segmentation using FCM, KM, and SOM across five color spaces, presenting visual results in Table-5, 6, 7 and numerical data in Tables 8, 9, 10. FCM and KM excel in the CIE Lab color space, while SOM performs well with HSI and HSV. The most effective clustering-color space pairs are FCM-CIELab, KM-CIELab, SOM-HSI, and SOM-HSV, emphasizing the importance of proper technique and color space selection for WBC segmentation.

Table 2: Segmenting Nuclei with Cluster Analysis in Various Color Spaces for Figure 2(b)

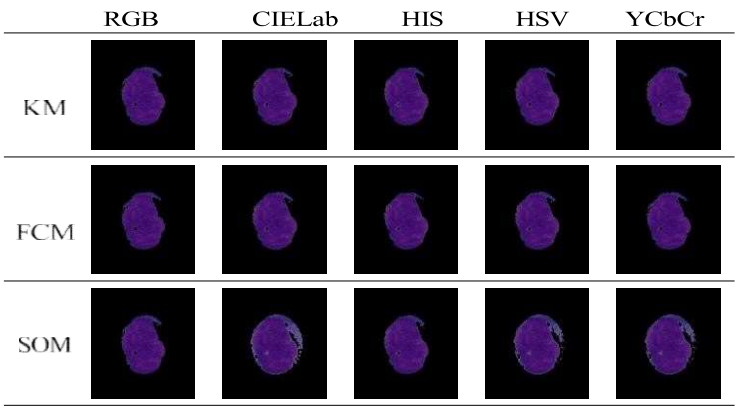

Table 6: Segmentation of Nucleus with Cytoplasm using Clustering Techniques in Various Color Spaces for Fig. 2(a)

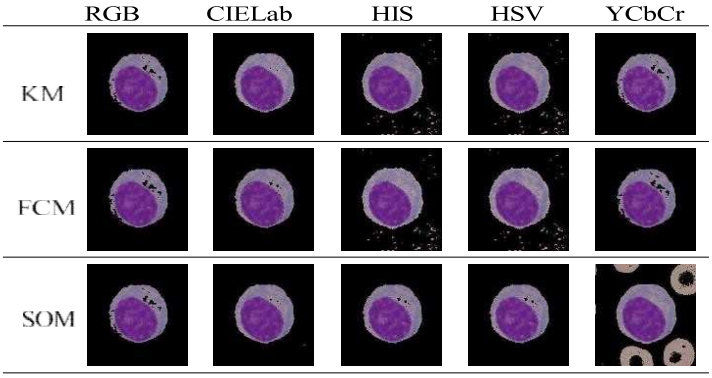

Table 3: Quality Parameters for FCM over different Color Spaces for nucleus detection.

Method	Accuracy	Recall	Precision	MCC	Dice	Jaccard	Specitivity
RGB	0.9839	0.9636	0.9602	0.9513	0.9610	0.9255	0.9870
CIELab	**0.9862**	0.9547	**0.9851**	**0.9560**	**0.9643**	**0.9314**	0.9927
HSI	0.9741	0.9026	0.9849	0.9265	0.9396	0.8894	**0.9963**
HSV	0.9801	0.9326	0.9742	0.9404	0.9520	0.9100	0.9930
YCbCr	0.9796	**0.9682**	0.9440	0.9421	0.9535	0.9127	0.9803

Table 4: Quality Parameters for KM over different Color Spaces for nucleus detection

Method	Accuracy	Recall	Precision	MCC	Dice	Jaccard	Specifivity
RGB	0.9831	0.9617	0.9596	0.9496	0.9601	0.9241	0.9872
CIELab	0.9858	0.9526	0.9818	0.9565	0.9644	0.9332	0.9944
HSI	**0.9844**	0.9478	0.9812	**0.9524**	**0.9616**	0.9268	**0.9952**
HSV	0.9825	0.9436	**0.9721**	0.9464	0.9567	**0.9183**	0.9922
YCbCr	0.9812	**0.9520**	0.9640	0.9456	0.9569	0.9190	0.9900

Table 5: Quality Parameters for SOM over different Color Spaces for nucleus detection.

Method	Accuracy	Recall	Precision	MCC	Dice	Jaccard	Specitivity
RGB	0.9801	0.9419	0.9818	0.9482	0.9604	0.9246	**0.9932**
CIELab	0.9471	0.9360	0.9179	0.8893	0.9195	0.8770	0.9505
HSI	**0.9844**	**0.9663**	0.9737	**0.9593**	**0.9694**	**0.9408**	**0.9903**
HSV	**0.9844**	0.9662	**0.9739**	**0.9593**	**0.9694**	**0.9408**	**0.9903**
YCbCr	0.8318	0.8759	0.7110	0.6688	0.7670	0.6706	0.8149

Table 8: Quality Metrics for Fuzzy C-Means in Various Color Spaces for Nucleus and Cytoplasm Detection

Method	Accuracy	Recall	Precision	MCC	Dice	Jaccard	Specitivity
RGB	0.9646	0.9414	0.9513	0.9215	0.9408	0.8939	0.9722
CIELab	**0.9763**	**0.9815**	**0.9588**	**0.9407**	**0.9555**	**0.9156**	**0.9842**
HSI	**0.9763**	0.9812	0.9327	0.9405	**0.9555**	**0.9156**	0.9736
HSV	0.9755	**0.9881**	0.9217	0.9379	0.9534	0.9120	0.9705
YCbCr	0.9599	0.9344	0.9407	0.9096	0.9314	0.8810	0.9700

Table 9: Quality Metrics for KM in Various Color Spaces for Nucleus and Cytoplasm Detection.

Method	Accuracy	Recall	Precision	MCC	Dice	Jaccard	Specitivity
RGB	0.9812	0.9477	0.9810	0.9515	0.9633	0.9296	**0.9929**
CIELab	**0.9850**	0.9649	0.9772	**0.9608**	**0.9705**	**0.9430**	0.9915
HSI	0.9754	**0.9803**	0.9311	0.9386	0.9539	0.9127	0.9726
HSV	0.9800	0.9788	0.9487	0.9495	0.9630	0.9289	0.9789
YCbCr	0.9799	0.9424	**0.9812**	0.9480	0.9604	0.9245	**0.9929**

Table 10: Quality Metrics for SOM in Various Color Spaces for Nucleus and Cytoplasm Detection

Method	Accuracy	Recall	Precision	MCC	Dice	Jaccard	Specitivity
RGB	0.9801	0.9419	0.9818	0.9482	0.9604	0.9246	**0.9932**
CIELab	0.9471	0.9360	0.9179	0.8893	0.9195	0.8770	0.9505
HSI	**0.9844**	**0.9663**	0.9737	**0.9593**	**0.9694**	**0.9408**	**0.9903**
HSV	**0.9844**	0.9662	**0.9739**	**0.9593**	**0.9694**	**0.9408**	**0.9903**
YCbCr	0.8318	0.8759	0.7110	0.6688	0.7670	0.6706	0.8149

5 Conclusion and Future works

This paper explores clustering-based techniques for segmenting white blood cells (WBCs) in Acute Lymphoblastic Leukemia (ALL) images, using various color spaces to enhance accuracy. Fuzzy C-Means (FCM) and K-Means (KM) with CIELab showed optimal results for nucleus and whole WBC segmentation. Self-Organizing Maps (SOM) with HSI excelled in nucleus segmentation, while HSI and HSV with SOM performed well for whole WBCs.

These findings emphasize that the choice of color space significantly impacts segmentation efficacy in different clustering approaches, highlighting the need for a tailored pairing of clustering method and color space.

The study also outlines potential future research directions, including:

- Explore advanced clustering techniques, including Rough-Fuzzy clustering, various Fuzzy clustering variants, and nature-inspired optimization algorithms (NIOA), to improve WBC segmentation.
- Investigate the use of diverse NIOAs, expanding beyond distance-based objective functions, to broaden the scope of research in WBC segmentation.
- Focus on optimizing color spaces for WBC segmentation, including under- utilized ones, and explore hybrid color spaces and color component-based segmentation to address illumination challenges.

In conclusion, this study underscores the significance of combining ap- propriate clustering techniques with suitable color spaces for effective WBC segmentation. It suggests avenues for future research to advance the field, encompassing the exploration of advanced clustering methods, diverse objective functions for NIOAs, and innovative approaches to leveraging color spaces for segmentation improvement.

Table 7: Segmentation of Nucleus with Cytoplasm using Clustering Techniques in Various Color Spaces for Fig. 2(b)

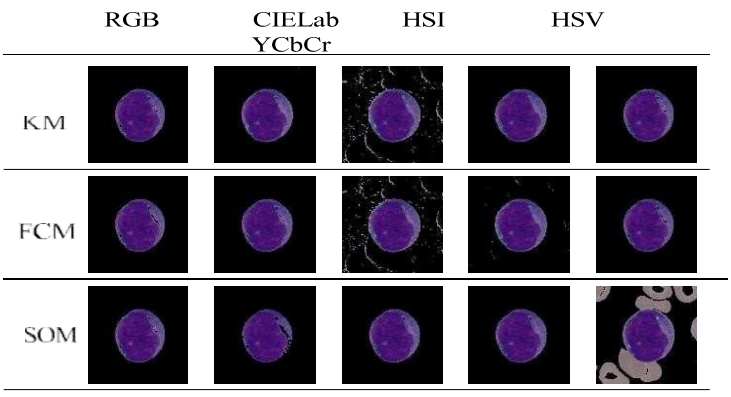

6 References

[1] Ajala Funmilola, A., Oke, O., Adedeji, T., Alade, O., Adewusi, E.: Fuzzy kc-means clustering algorithm for medical image segmentation. Journal of information Engineering and Applications, ISSN 22245782, 2225–0506 (2012).

[2] Alagarsamy, S., Govindaraj, V., et al.: Automated brain tumor segmentation for mr brain images using artificial bee colony combined with interval type-ii fuzzy technique. IEEE Transactions on Industrial Informatics (2023)

[3] Chen, J.: Survey of evaluation methods and metrics for face clustering. In: 2023 IEEE 13th International Conference on Electronics Information and Emergency Communication (ICEIEC), pp. 181–186. IEEE (2023)

[4] Chicco, D., Jurman, G.: The matthews correlation coefficient (mcc) should replace the roc auc as the standard metric for assessing binary classification. Biodata Mining **16**(1), 1–23 (2023)

[5] Dhal, K.G., Ray, S., Barik, S., Das, A.: Illumination-free clustering using improved slime mould algorithm for acute lymphoblastic leukemia image segmentation. Journal of Bionic Engineering pp. 1–19 (2023)

[6] Gurcan, M.N., Boucheron, L.E., Can, A., Madabhushi, A., Rajpoot, N.M., Yener, B.: Histopathological image analysis: A review. IEEE reviews in biomedical engineering **2**, 147–171 (2009)

[7] He, Y., Yang, G., Ge, R., Chen, Y., Coatrieux, J.L., Wang, B., Li, S.: Geometric visual similarity learning in 3d medical image self-supervised pre-training. In: Proceedings of the IEEE/CVF Conference on Computer Vision and Pattern Recognition, pp. 9538– 9547 (2023)

[8] Hegde, R.B., Prasad, K., Hebbar, H., Singh, B.M.K.: Comparison of traditional image processing and deep learning approaches for classification of white blood cells in peripheral blood smear images. Biocybernetics and Biomedical Engineering **39**(2), 382–392 (2019)

[9] Irshad, H., Veillard, A., Roux, L., Racoceanu, D.: Methods for nuclei detection, segmentation, and classification in digital histopathology: a review—current status and future potential. IEEE reviews in biomedical engineering **7**, 97–114 (2013)

[10] Labati, R.D., Piuri, V., Scotti, F.: All-idb: The acute lymphoblastic leukemia image database for image processing. In: 2011 18th IEEE international conference on image processing, pp. 2045–2048. IEEE (2011)

[11] Rawat, J., Singh, A., Bhadauria, H., Virmani, J., Devgun, J.S.: Computer assisted classification framework for prediction of acute lymphoblastic and acute myeloblastic leukemia. Biocybernetics and Biomedical Engineering **37**(4), 637–654 (2017)

[12] Ren, Z., Kong, X., Zhang, Y., Wang, S.: Ukssl: Underlying knowledge based semi- supervised learning for medical image classification. IEEE Open Journal of Engineering in Medicine and Biology (2023)

[13] Rezatofighi, S.H., Soltanian-Zadeh, H.: Automatic recognition of five types of white blood cells in peripheral blood. Computerized Medical Imaging and Graphics **35**(4), 333–343 (2011)

[14] Shahin, A.I., Guo, Y., Amin, K.M., Sharawi, A.A.: White blood cells identification system based on convolutional deep neural learning networks. Computer methods and programs in biomedicine **168**, 69–80 (2019)

[15] Suryani, E., Palgunadi, S., Pradana, T.N., et al.: Classification of acute myelogenous leukemia (aml m2 and aml m3) using momentum back propagation from watershed distance transform segmented images. In: Journal of Physics: Conference Series, vol. 801, p. 012044. IOP Publishing (2017)

[16] Swanson, K., Wu, E., Zhang, A., Alizadeh, A.A., Zou, J.: From patterns to patients: Advances in clinical machine learning for cancer diagnosis, prognosis, and treatment. Cell (2023)

[17] Tang, T., Zhang, R., Lin, K., Li, F., Xia, X.: Sm- rnet: A scale-aware-based multi- attention guided reverse network for pulmonary nodules segmentation. IEEE Transac- tions on Instrumentation and Measurement (2023)

[18] Zhang, N., Jiang, Z., Li, J., Zhang, D.: Multiple color representation and fusion for diabetes mellitus diagnosis based on back tongue images. Computers in Biology and Medicine **155**, 106652 (2023)

[19] Zhang, W., Cao, Y., Hu, X., Mi, J., Zhang, P., Mukhopadhyay, S.C., Li, Y., Liu, Z.: Iat: A full-scale ivus analysis toolbox based on deep learning algorithms for clinical diagnosis. IEEE Transactions on Instrumentation and Measurement **72**, 1–15 (2023)